Supplementary material to "Simulation of Auger decay dynamics in the hard x-ray regime: HCl as showcase"

G. Goldsztejn,[1] R. Guillemin,[2] T. Marchenko,[2] O. Travnikova,[2] D. Céolin,[3] L. Journel,[2] M. Simon,[2] M. N. Piancastelli,[2,4] and R. Püttner[5]

[1]*Institut des Sciences Moléculaires d'Orsay (ISMO), CNRS, Univ. Paris-Sud, Université Paris-Saclay, F-91405 Orsay (France)*
[2]*Sorbonne Université, CNRS, Laboratoire de Chimie Physique-Matière et Rayonnement, LCPMR, F-75005 Paris Cedex 05, France*
[3]*Synchrotron SOLEIL, l'Orme des Merisiers, Saint-Aubin, F-91192 Gif-sur-Yvette Cedex, France*
[4]*Department of Physics and Astronomy, Uppsala University, SE-75120 Uppsala, Sweden*
[5]*Fachbereich Physik, Freie Universität Berlin, Arnimallee 14, D-14195 Berlin, Germany.*

The main idea of this supplementary material is to provide more detailed information on the derivation of the equations given in the main text.

I. FROM THE DOUBLE DIFFERENTIAL CROSS SECTION TO RESONANT AND NORMAL AUGER

In this section we want to discuss the lineshapes and intensities from resonant and normal Auger spectra by starting from the generalized Kramers-Heisenberg formula. Schematic pictures of the two processes are shown in Fig. 1 of the main text. Here we distinguish between final states of infinite lifetime and finite lifetime for the final state of the process. Finally we show a comparison of the simulated and measured partial electron yield spectra.

A. Final states with infinite lifetime

Let us start with the situation of an infinite experimental resolution and a stable final state, i.e. with infinite lifetime. In this case the double differential cross section is described in its general form by [1]

$$\sigma(\omega,\omega') \propto \sum_f |F_f|^2 \cdot \delta(\omega-\omega'-\omega_{fo}) \tag{1}$$

with

$$F_f = \sum_c \frac{\langle\Psi_f|\mathbf{Q}|\Psi_c\rangle\langle\Psi_c|\mathbf{D}|\Psi_o\rangle}{\omega-\omega_{co}+i\Gamma_c}. \tag{2}$$

Here, ω is the energy of the incoming photon, ω' the energy of the outgoing photon or electron(s), ω_{co} the energy difference between the ground state $|o\rangle$ and the core-excited state $|c\rangle$, ω_{fo} the energy difference between the ground state $|o\rangle$ and the core-excited state $|f\rangle$, $\mathbf{D}$ the dipole operator for the excitation, $\mathbf{Q}$ the decay operator (Coulomb operator for Auger decay or dipole operator for RIXS) and Γ_c the half width at half maximum (HWHM) of the core-hole lifetime broadening.

Equation 1 can be applied to the resonant and normal Auger process. In the resonant Auger process in the first step an electron is excited from a core hole to an unoccupied orbital $n\ell$ below the ionization threshold. This neutral excited state can be considered as consisting of a cation A^+ with an electron in the orbital bound to it. In the next step the cation A^+ undergoes an Auger decay and forms a dication A^{2+} while the excited electron remains in a bound orbital. This process can be described as $g.s. \rightarrow A^+n\ell \rightarrow A^{2+}n\ell\epsilon'\ell'$ with $g.s.$ being the ground state and $\epsilon'\ell'$ being the Auger electron. In contrast to this, to observe the normal Auger process, the core electron is promoted in the first step into the continuum $\epsilon\ell$. After this, the cation decays to an dication end emits an Auger elctron. Here the process can be described at $g.s. \rightarrow A^+\epsilon\ell \rightarrow A^{2+}\epsilon\ell\epsilon'\ell'$.

In the following we shall first focus on the resonant Auger. Furthermore, we restrict the considerations to only one core-excited intermediate state $A^+n\ell$ and one final state $A^{2+}n\ell\epsilon'\ell'$. In this case eqn. 2 simplifies to

$$F_f = \frac{\langle A^{2+}n\ell\epsilon'\ell'|\mathbf{Q}|A^+n\ell\rangle\langle A^+n\ell|\mathbf{D}|\Psi_o\rangle}{\omega-\omega_{co}+i\Gamma_c} \tag{3}$$

and we obtain with $\mathbf{Q_{res}} = \langle A^{2+} n\ell\epsilon'\ell'|\mathbf{Q}|A^+ n\ell\rangle$ as well as $\mathbf{D_{res}} = \langle A^+ n\ell|\mathbf{D}|\Psi_o\rangle$ for the partial differential cross section

$$\begin{aligned}\sigma(\omega,\omega') &\propto \left|\frac{\mathbf{Q_{res}}\mathbf{D_{res}}}{\omega-\omega_{co}+i\Gamma_c}\right|^2 \cdot \delta(\omega-\omega'-\omega_{fo}) \\ &\propto \frac{\Gamma_c}{\pi}\frac{|\mathbf{Q_{res}}\mathbf{D_{res}}|^2}{(\omega-\omega_{co})^2+\Gamma_c^2}\cdot\delta(\omega-\omega'-\omega_{fo}).\end{aligned} \tag{4}$$

In this equation the δ function represents the energy conservation and defines the kinetic energy ω' of the resonant Auger electron as a function of the incoming photon. In the last line an additional factor $\frac{\Gamma_c}{\pi}$ is added to obtain a Lorentzian function normalised to unity. By neglecting experimental broadenings, i.e. photon bandwidth and analyser resolution, the spectrum consists of a δ-like peak at the energy $\omega' = \omega - \omega_{fo}$, see black vertical lines in panel (a) of Fig. 2 in the main text. The matrix element $\mathbf{D_{res}}$ in eqn. 4 describes the resonant excitation and the matrix element $\mathbf{Q_{res}}$ the Auger decay. Due to the finite lifetime Γ_c the process can resonate over a larger energy range. The intensity of the δ-like peak varies with ω and the variation is described with a Lorentzian function, see Fig. 1(a) and as red curve in Fig. 2(a) of the main text, which is derived from $\left((\omega-\omega_{co})^2+\Gamma_c^2\right)^{-1}$ in eqn. 4. In summary, $|F_f|^2$ gives the probability of the process as a function of the photon energy ω and the δ-function defines the energy ω' of the outgoing Auger electron as a function of the incoming photon.

In the next step we shall consider the normal Auger process subsequent to a photoionization process, i.e. $g.s. \rightarrow A^+\epsilon\ell \rightarrow A^{2+}\epsilon\ell\epsilon'\ell'$. In Fig. 1(b) of the main text it can be seen that the photon energy ω is not in the Lorentzian distribution of the core-hole state $|c\rangle$, i.e. the process is non-resonant. Instead, the process leads to two outgoing electrons, namely the photoelectron with a kinetic energy ω_P and the Auger electron with a kinetic energy ω_A. Note that ω_P and ω_A are the actual energies of the emitted electrons, but not the peak maxima in the photoelectron and the Auger spectrum. This leads to the relation $\omega' = \omega_P + \omega_A$, which can only be varified in photoelectron-Auger electron coincidence spectra.

In the next step we define $\tilde{\omega} = \omega - \omega_P$. The probability of the ionization process is than given by $\tilde{\omega} - \omega_{co}$ which is the detuning of photoelectron from the peak maximum. This is equivalent to a Lorentzian profile around $\omega - \omega_{co}$ visible in the photoabsorption spectrum, which governs the excitation probability in the resonant Auger process. Moreover, the amplitudes for the photoelectron and the normal Auger process have to be used. This leads with $\mathbf{D_{nor}} = \langle A^+\epsilon\ell|\mathbf{D}|\Psi_o\rangle$ and $\mathbf{Q_{nor}} = \langle A^{2+}\epsilon\ell\epsilon'\ell'|\mathbf{Q}|A^+\epsilon\ell\rangle$ to

$$\begin{aligned}\sigma(\omega,\omega_A) &\propto \left|\frac{\mathbf{Q_{nor}}\mathbf{D_{nor}}}{\tilde{\omega}-\omega_{co}+i\Gamma_c}\right|^2 \cdot \delta(\tilde{\omega}-\omega_A-\omega_{fo}) \\ &\propto \frac{\Gamma_c}{\pi}\frac{|\mathbf{Q_{nor}}\mathbf{D_{nor}}|^2}{(\tilde{\omega}-\omega_{co})^2+\Gamma_c^2}\cdot\delta(\tilde{\omega}-\omega_A-\omega_{fo})\end{aligned} \tag{5}$$

for the description of the process for the case of an outgoing Auger electron with the energy ω_A. Here the δ-function is derived from $\delta(\omega-\omega'-\omega_{fo})$ by using $\omega' = \omega_P + \omega_A$ and $\tilde{\omega} = \omega - \omega_P$. Note that the photon energy ω contributes implicitly to the matrix element $\mathbf{D_{nor}}$ for the photoionization process.

Equation 6 is obviously very similar to eqn. 4. However, contrary to ω is eqn. 4 the quantity $\tilde{\omega}$ in eqn. 6 can have different values around ω_{co} so that one has to integrate over $\tilde{\omega}$, i.e.

$$\begin{aligned}\sigma(\omega,\omega_A) &\propto \int d\tilde{\omega}\frac{\Gamma_c}{\pi}\frac{|\mathbf{Q_{nor}}\mathbf{D_{nor}}|^2}{(\tilde{\omega}-\omega_{co})^2+\Gamma_c^2}\cdot\delta(\tilde{\omega}-\omega_A-\omega_{fo}) \\ &= \frac{\Gamma_c}{\pi}\frac{|\mathbf{Q_{nor}}\mathbf{D_{nor}}|^2}{(\omega_A+\omega_{fo}-\omega_{co})^2+\Gamma_c^2} \\ &= \frac{\Gamma_c}{\pi}\frac{|\mathbf{Q_{nor}}\mathbf{D_{nor}}|^2}{(\omega_A-\omega_{cf})^2+\Gamma_c^2}\end{aligned} \tag{6}$$

with $\omega_{cf} = \omega_{co} - \omega_{fo}$. Obviously, $\sigma(\omega,\omega_A)$ is described by a Lorentzian function around the energy difference ω_{fc} between the core-hole and the final state, see Fig. 2(c) of the main text.

It is also important to understand that different values of $\tilde{\omega}$ lead to different values of ω_P and ω_A, i.e. to different final states of the Auger decay which include not only the dication A^{2+} but also both outgoing electrons.

It should be mentioned that the sum (or in case of a continuum of intermeditate states the integral) over c in equation 2 can lead to lifetime interference contributions, see e.g. discussion around eqn. 9 of the main text. These contributions occur if one particular final state can be populated by different intermediate states. However, in the present case the photoelectron $\epsilon\ell$ is part of the Auger final state so that for each final state $|f\rangle = |A^{2+}\epsilon\ell\epsilon'\ell'\rangle$ there is only one possible intermediate state, namely $|c\rangle = |A^+\epsilon\ell\rangle$ so that no lifetime interference can occur.

B. Final states with finite lifetime

Up to now we have assumed that the Auger final state has a infinite lifetime. This is a reasonable approximation for the Auger final states subsequent to the decay of shallow core-hole states. Contrary to this the final states after the decay of deeper core levels (e.g. Ar $1s^{-1} \rightarrow 2p^{-2}$) possess non-negligible lifetime broadenings which have to be taken into account. As a result, the accessible energy levels show a Lorentzian-like distribution with a width Γ_f around the energy of the final state; here Γ_f is the lifetime broadening of the final state (HWHM). Once again, we have to tread resonant and normal Auger separately.

For resonant Auger we have to start with the second line of eqn. 4. Due to the finite lifetime the energy difference between the initial and the final state is not a fixed value ω_{fo}, but shows a Lorentzian-like distribution around ω_{fo}. As a result, the possible final state energies can be described in a normalized form with

$$L(\tilde{\omega}_{fo}) = \frac{\Gamma_f}{\pi((\omega_{fo} - \tilde{\omega}_{fo})^2 + \Gamma_f^2)}. \tag{7}$$

To take this distribution into account the second line of eqn. 4 has to be convoluted with the Lorentz-distribution and one obtains

$$\begin{aligned} \sigma(\omega, \omega') \;\propto\; & \int d\tilde{\omega}_{fo} \frac{\Gamma_c}{\pi} \frac{|\mathbf{Q_{res}}\mathbf{D_{res}}|^2}{(\omega - \omega_{co})^2 + \Gamma_c^2} \times \\ & \delta(\omega - \omega' - \tilde{\omega}_{fo}) \cdot \frac{\Gamma_f}{\pi((\omega_{fo} - \tilde{\omega}_{fo})^2 + \Gamma_f^2)} \\ = \; & \frac{\Gamma_c}{\pi} \frac{|\mathbf{Q_{res}}\mathbf{D_{res}}|^2}{(\omega - \omega_{co})^2 + \Gamma_c^2} \times \\ & \frac{\Gamma_f}{\pi((\omega_{fo} - \omega - \omega')^2 + \Gamma_f^2)}. \end{aligned} \tag{8}$$

Obviously, the obtained result is a product of the intensity factor already present in eqn. 5 and a Lorentzian function with a width Γ_f. From this follows that the kinetic energy of the Auger electron, ω', can be described by a Lorentzian function with a maximum at $\omega_{fo} - \omega$, i.e. the maximum depends on the photon energy, and a width of Γ_f, see black curve in Fig. 2(c) of the main text. The third line of the equation defines the red Lorentzian lineshape in Fig. 2(c) of the main text which indicates the intensity of the black Lorentzian curve.

In the next step we shall consider the normal Auger decay. In the last line of eqn. 6 it can be seen that the kinetic energy of the Auger electron follows a Lorentzian distribution around ω_{cf}. However, in case of a final state $|f\rangle$ with finite lifetime broadening Γ_f the energy difference $\tilde{\omega}_{cf}$ between the core-ionized state and the final state is not fixed, but follows a Lorentzian distribution around ω_{cf}, i.e.

$$L(\omega_{cf}) = \frac{\Gamma_f}{\pi((\omega_{cf} - \tilde{\omega}_{cf})^2 + \Gamma_f^2)}. \tag{9}$$

To take this into account, the cross section in eqn. 6 has to be convoluted with the distribution in eqn. 9, i.e.

$$\begin{aligned} \sigma(\omega, \omega_A) \;\propto\; & \int d\tilde{\omega}_{cf} \frac{\Gamma_c |\mathbf{Q_{nor}}\mathbf{D_{nor}}|^2}{\pi((\omega_A - \tilde{\omega}_{cf})^2 + \Gamma_c^2)} \times \\ & \frac{\Gamma_f}{\pi((\omega_{cf} - \tilde{\omega}_{cf})^2 + \Gamma_f^2)} \\ = \; & \frac{\Gamma_t |\mathbf{Q_{nor}}\mathbf{D_{nor}}|^2}{\pi((\omega_A - \omega_{cf})^2 + \Gamma_t^2)}. \end{aligned} \tag{10}$$

As displayed in Fig. 2(d) of the main text, the result of the convolution is also a Lorentzian function, however, with a larger width $\Gamma_t = \Gamma_f + \Gamma_c$, i.e. the sum of the lifetime broadening of the core-hole and the final state.

II. THE MOLECULAR CASE

In the Born-Oppenheimer's approximation, we can factorise the electronic and nuclear degrees of freedom such that Ψ_i from the equation 1 can be rewritten as $|\Psi_i\rangle = |\Phi_i\rangle|\chi_i\rangle$. $|\Phi_i\rangle$ represents the electronic wavefunction as defined

previously and $|\chi_i\rangle$ is the nuclear wavefunction. In this approximation eqn. 1 can be rewritten as

$$\sigma(\omega,\omega') \propto \sum_f \left| \sum_c \frac{\langle\Phi_f|Q|\Phi_c\rangle\langle\chi_f|\chi_c\rangle\langle\Phi_c|D|\Phi_o\rangle\langle\chi_c|\chi_o\rangle}{\omega-\omega_{co}+i\Gamma_c} \right|^2 \Delta(\omega-\omega'-\omega_{fo},\Gamma_f). \tag{11}$$

In this context $\Delta(\omega-\omega'-\omega_{fo},\Gamma_f$ describes the spectral lineshapes and has to be derived in line with the arguments above according to the the situation, i.e. resonant or normal Auger as well as the lifetime of the final states.

Let us now focus on the overlap integrals of the nuclear wavefunctions and rewrite 11 with $\mathbf{D_{el}} = \langle\Phi_c|D|\Phi_o\rangle$ and $\mathbf{Q_{el}} = \langle\Phi_f|Q|\Phi_c\rangle$ as

$$\sigma(\omega,\omega') \propto \sum_f |\mathbf{Q_{el}}|^2|\mathbf{D_{el}}|^2 \left| \sum_c \frac{\langle\chi_f|\chi_c\rangle\langle\chi_c|\chi_o\rangle}{\omega-\omega_{co}+i\Gamma_c} \right|^2 \Delta(\omega-\omega'-\omega_{fo},\Gamma_f). \tag{12}$$

Note that with writing $|\mathbf{Q_{el}}|^2$ and $|\mathbf{D_{el}}|^2$ before the sum we make the assumption of only one electronic intermediate state, i.e. the different intermediate states are all formed by different levels of the nuclear motion. To apply eqn. 12 for the vibrational states of electronic transitions, the nuclear wavefunctions χ_i have to be described according to the case that they describe bound or dissociative molecular states. In principle, the transitions described by the matrix elements $\langle\chi_f|\chi_c\rangle$ and $\langle\chi_c|\chi_o\rangle$ can have different characters depending on the bond character of the potential energy curves.

In the following we shall first discuss the vibrational profiles of transitions between two states, where we have to distinguish between bound-bound transitions, bound-dissociative transitions and dissociative-dissociative transitions. After this we will discuss the entire excitation and decay process, which includes three different states. Since we only consider processes which involve the ground state, we here have to distinguish four cases, namely bound-bound-bound transitons, bound-bound-dissociative transitions, bound-dissociative-bound transitions and bound-dissociative-dissociative transitions.

A. Bound-bound-transitions

We will start the discussion with transitions between two bound states $|b\rangle$ and $|b'\rangle$. Such transitions can occur between the ground and the core-hole state as well as between the core-hole and the final state, i.e. the vibrational overlap matrix elements $\langle\chi_b|\chi_{b'}\rangle$ can represent the matrix elements $\langle\chi_f|\chi_c\rangle$ and $\langle\chi_c|\chi_0\rangle$. For bound states the potential energy curves can be described with Morse potentials described with three parameters: equilibrium distance R_0, vibrational energy $\hbar\omega$, and anharmonicity $x\hbar\omega$. The simple case of an harmonic oscillator is obtained with $x\hbar\omega = 0$. In case of Morse potentials the vibrational overlap matrix elements $\langle\chi_b|\chi_{b'}\rangle$ can be obtained by following the methods of Ory, Gittleman, and Maddox [2] as well as Halmann and Laulich [3]. Details of a corresponding fit approach are discussed in Ref. [4].

B. Bound-dissociative-transitions

In the following discussion of transitions between a bound state $|b\rangle$ and a dissociative state $|d\rangle$ we have to calculate the Franck-Condon factor $\langle\chi_d|\chi_{b0}\rangle$ where $|\chi_d\rangle$ is the continuum wavefunction for the energy E_d and $|\chi_{b0}\rangle$ the wavefunction of the vibrational ground state of the state $|b\rangle$. Bound-dissociative transitions can occur between the ground and the core-hole state as well as between the core-hole and the final state, so that the matrix elements $\langle\chi_d|\chi_{b0}\rangle$ can represent the matrix elements $\langle\chi_f|\chi_c\rangle$ and $\langle\chi_c|\chi_0\rangle$. The potential energy curves and the nuclear wavefunctions are presented in Fig. 3 of the main text.

For the calculation we assume that the slope of the dissociative potential energy curve is constant. Moreover, we assume that the bound state is the initial state and that only the vibrational ground state of the bound state is populated. By applying an harmonic oscillator potential for the bound state the vibrational wavefunction is given by

$$\chi_{b0}(x) = \left(\frac{1}{\pi a_0^2}\right)^{1/4} \exp\left[-\frac{1}{2}\left(\frac{x}{a_0}\right)^2\right] \tag{13}$$

with $a_0 = \left(\frac{\hbar}{\mu\omega_0}\right)^{1/2}$. Here, μ is the reduced mass, ω_0 the vibrational frequency, and a_0 the average deviation of $x = R - R_0$ with R_0 being the equilibrium distance.

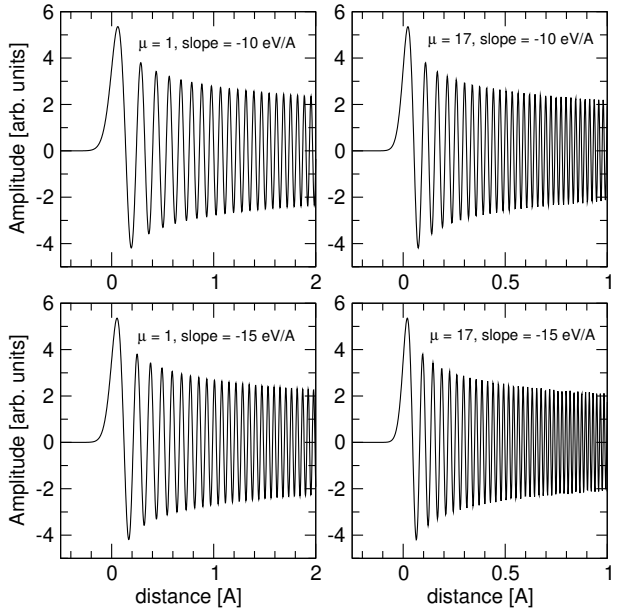

FIG. 1: Airy functions for reduced masses $\mu = 1$ and 15 m_{proton} as well as slopes of -10 and -15 eV/Å. The internuclear distances are given relative to the classical turning point.

As stated above, we approximate the dissociative potential energy curve with a linear function, i.e. $V(x) = -F_d x$ with F_d being the slope of the dissociative state. The corresponding Schrödinger equation to be solved is given by

$$\frac{d^2\chi_d}{dx^2} + \frac{\mu}{\hbar^2}\left(E + F_d x\right)\chi_d = 0, \tag{14}$$

with μ being the reduced mass of the molecule. With the substitution [5]

$$\zeta = \left(x + \frac{E}{F_d}\right)\left(\frac{2\mu F_d}{\hbar^2}\right)^{1/3} \tag{15}$$

on obtains the Airy-equation

$$\frac{d^2\chi_d}{d\zeta^2} + \zeta\chi_d = 0. \tag{16}$$

This differential equation is solved by the Airy functions $Ai(\zeta)$ and $Bi(\zeta)$. The latter function is not square-intelerable and can be neglected so that the relevant solution is given by the Airy functions $Ai(\zeta)$. In this way, the solution of the initial Schrödinger equation (eqn. 14 is given by

$$\chi_{d,E}(x) = \frac{(2\mu)^{1/3}}{\hbar^{2/3}F_d^{1/6}} Ai\left[-\frac{(2\mu F_d)^{1/3}}{\hbar^{2/3}}\left(x + \frac{E}{F_d}\right)\right]. \tag{17}$$

Obviously, the wave functions for different energies E are shifted along the internuclear coordinate x while changes in the slope F_d as well as in the reduced mass μ influence the oscillations of the function. In order to get an idea about the length of the oscillations Fig. 1 shows the Airy functions for the $\mu = 1$ m_{proton} and $\mu = 17$ m_{proton} which represents e.g. HCl and Cl_2, respectively. For both masses typical slopes of -10 eV/Å and -15 eV/Å were used in the calculations.

With the substitutions $a = \frac{E}{F_d}$ and $\alpha = \left(-\frac{(2\mu F_d)^{1/3}}{\hbar^{2/3}}\right)^{-1}$ one obtains

$$\chi_{d,E}(x) = \frac{1}{\alpha F_d^{1/2}} Ai\left[\frac{x+a}{\alpha}\right]. \tag{18}$$

For $\frac{x+a}{\alpha} < 0$ the Airy function decreases quickly and for $\frac{x+a}{\alpha} > 0$ it oscillates strongly. Based on this, the Franck-Condon factor can be approximated to

$$\langle \chi_d | \chi_{b0} \rangle \cong \left(\frac{2\mu\alpha^3}{\sqrt{\pi} a_0} \right)^{1/2} \times \exp \left[-\frac{1}{2} \left(\frac{\Delta E_d}{\gamma_d} \right)^2 \right] \tag{19}$$

with $\Delta E_d = E - F_d\alpha$ and $\gamma_d = F_d a_0$ [1]. Here E is the the energy relative to $U_d(R_0)$.

Obviously, the dependence of the Franck-Condon factors on the energy E can be described with a Gaussian distribution as for the nuclear wavefunction in the ground state. Because of this, the behaviour of the Franck-Condon factors can be obtained by approximating the Airy functions by δ functions, which peak at the classical turning point. Note that in this way the energy shift $F_d\alpha$ can not be reproduced. One should also mention that the approximation of the Airy function by a δ function is not obvious since the width of the first oscillation of the Airy function is comparable to the width of the nuclear ground state, see Fig. 3 of the main text. However, it has been shown that the Franck-Condon factors of the exact solution and the approximation deviate only very slightly, see Herzberg [6]. The approximation of the Airy functions with δ functions allow also a derivation of the Franck-Condon factors for higher vibrational states in the bound potential, see e.g. [7].

C. Dissociative-dissociative-transitions

In the following we want to consider transitions between two dissociative states $|d\rangle$ and $|d\rangle'$. Such transitions can occur in the present study only between the core-excited and the final states. In the calculation of the vibrational matrix elements $\langle \chi_d | \chi'_d \rangle$, the nuclear wavefunctions can be described with Airy functions, which allows to use [8]

$$\frac{1}{|\alpha\beta|} \int_{-\infty}^{\infty} Ai\left[\frac{x+a}{\alpha}\right] Ai\left[\frac{x+b}{\beta}\right] dx = \begin{cases} \delta(b-a) & \text{if } \alpha = \beta \\ \frac{1}{|\beta^3-\alpha^3|^{1/3}} Ai\left[\frac{b-a}{(\beta^3-\alpha^3)^{1/3}}\right] & \text{if } \beta > \alpha. \end{cases} \tag{20}$$

Note that $\alpha = \beta$ if the slopes of the two potential energy curves involved are equal. This assumption is generally assumed to be valid for Resonant Inelastic X-ray Scattering (RIXS) spectra. In this case a nuclear wavefunction in the electronic final state is populated via one nuclear wavefunction in the initial state. As a result of a excitation and decay process the intermediate nuclear state is always exactly known so that no vibrational lifetime interference occurs.

III. THE ENTIRE EXCITATION AND DECAY PROCESS

A. The bound-bound-bound case

In the case of bound-bound-bound transitons one can start with equation 12 by taking into account that the vibrational levels are all discrete. In this case the vibrational matrix elements $\langle \chi_f | \chi_c \rangle$ and $\langle \chi_c | \chi_o \rangle$ can be calculated by the approach given in section II A. Details on the simulation of bound-bound-bound transitions can be found in Refs. [9, 10].

B. The bound-dissociative-dissociative case

In the bound-dissociative-dissociative case the potential energy curves of the intermediate and the final state are approximated by linear slopes. Here we can distinguish between two cases, namely identical and different slopes for the two involved potential energy curves. The first case is realized in case of RIXS since here is one deep core hole in the intermediate and one shallow core hole in the final state. Since in both states only one core hole influences the valence shell the potential energy curves are expected to be very similar. The second case of different slopes is realized in Auger processes since here the number of core holes increase by one during the decay.

We start with eqn. 12 and assume a infinite lifetime for the final state. The overlap integral $\langle \chi_0 | \chi_c \rangle$ can be replace by eqn. 19. The treatment of the overlap integral $\langle \chi_c | \chi_f \rangle$ shows, however, differences for identical and different slopes, although the final results are identical.

In case of identical slopes we can use Airy functions for the continuum and obtain form the upper line of eqn. 20 as an exact result $\langle \chi_0 | \chi_c \rangle = \delta\left(\frac{\Delta E_c}{F_c} - \frac{\Delta E_f}{F_f}\right)$ with $F_c = F_f$. This δ-function ensures that a given final-state

nuclear wave function can be populated only via one given core-hole nuclear wavefunction so that vibrational lifetime interference can be ruled out. In contrast to this, the lower line of eqn. 20 shows that in case of different slopes of the potential energy curves a given final-state nuclear wave function can be populated can be populated via different core-hole nuclear wavefunction, i.e. vibrational lifetime interference cannot be strictly ruled out.

However, as discussed above, it was shown that for a bound-dissociative transition the Airy function can be replace by a δ function localized at the classical turning point. We now assume that this also works well for a dissociative-dissociative transition with different slopes for the potential energy curves, i.e.

$$|\chi_c\rangle = \delta(R - (R_0 - \frac{\Delta E_c}{F_c})) \quad \text{and} \quad |\chi_f\rangle = \delta(R - (R_0 - \frac{\Delta E_f}{F_f})). \tag{21}$$

Here, ΔE_i is the deviation of the energy from the potential energy curve at the equilibrium distance, $U_i(R_0)$ and F_i the slope of the potenial of the state $|\chi_i\rangle$. From this follows

$$\langle\chi_c|\chi_f\rangle = \int dR\ \delta(R - (R_0 - \frac{\Delta E_c}{F_c})) \cdot \delta(R - (R_0 - \frac{\Delta E_f}{F_f})) = \delta\left(\frac{\Delta E_c}{F_c} - \frac{\Delta E_f}{F_f}\right), \tag{22}$$

i.e. we obtain the same δ-function as in case of identical slopes for the potential energy curves. This means that once again a final state can be populated only by one intermediate state and vibrational lifetime interference is suppressed. We will now first solve the general Auger case and than specify for the RIXS case by using $F_f = F_c$. With the given information on the overlap integrals we can rewrite eqn. 12 as

$$\begin{aligned}
\sigma(\omega,\omega') \ &\propto \ \int d\Delta E_f \left| \frac{\int d\Delta E_c \exp\left[-\frac{1}{2}\left(\frac{\Delta E_c}{\gamma_c}\right)^2\right] \delta\left(\frac{\Delta E_c}{F_c} - \frac{\Delta E_f}{F_f}\right)}{\omega - \omega_{co}(R_0) - \Delta E_c + i\Gamma_c} \right|^2 \delta(\omega - \omega' - \omega_{fo}(R_0) - \Delta E_f) \\
&= \int d\Delta E_f \left| \frac{\exp\left[-\frac{1}{2}\left(\frac{\Delta E_f}{\gamma_f}\right)^2\right]}{\omega - \omega_{co}(R_0) - \frac{F_c}{F_f}\Delta E_f + i\Gamma_c} \right|^2 \delta(\omega - \omega' - \omega_{fo}(R_0) - \Delta E_f) \\
&= \frac{\exp\left[-\left(\frac{\omega-\omega'-\omega_{fo}(R_0)}{\gamma_f}\right)^2\right]}{(\omega - \omega_{co}(R_0) - \frac{F_c}{F_f}(\omega - \omega' - \omega_{fo}(R_0)))^2 + \Gamma_c^2}.
\end{aligned} \tag{23}$$

The integral $\int d\Delta E_c$ replaces the sum over c in equation 12 since in the present case there is a continuum of core-hole states. Moreover, $\omega_{co}(R_0)$, $\omega_{fo}(R_0)$, and $\omega_{cf}(R_0)$ represent the energy differences between the states at the equilibrium distance R_0. The integration over the different final states is represented by the integration $\int d\Delta E_f$.

As discussed in section I B in case of a resonant Auger decay to final states with finite lifetime, the δ-function in eqn. 23 has to be replace by a Lorentzian around $\omega - \omega' - \omega_{fo}(R_0) - \Delta E_f$ and a width Γ_f. In this case we obtain

$$\begin{aligned}
\sigma(\omega,\omega') \ &\propto \ \int d\Delta E_f \left| \frac{\int d\Delta E_c \exp\left[-\frac{1}{2}\left(\frac{\Delta E_c}{\gamma_c}\right)^2\right] \delta\left(\frac{\Delta E_c}{F_c} - \frac{\Delta E_f}{F_f}\right)}{\omega - \omega_{co}(R_0) - \Delta E_c + i\Gamma_c} \right|^2 \frac{\Gamma_f}{\pi((\omega - \omega' - \omega_{fo}(R_0) - \Delta E_f)^2 + \Gamma_f^2)} \\
&= \int d\Delta E_f \frac{\exp\left[-\left(\frac{\Delta E_f}{\gamma_f}\right)^2\right]}{(\omega - \omega_{co}(R_0) - \frac{F_c}{F_f}\Delta E_f)^2 + \Gamma_c^2} \times \frac{\Gamma_f}{\pi((\omega - \omega' - \omega_{fo}(R_0) - \Delta E_f)^2 + \Gamma_f^2)},
\end{aligned} \tag{24}$$

compare Ref. [11].

In the next step we simplify eqn. 23 by assuming the RIXS-case with $F_c = F_f$ and obtain

$$\sigma(\omega,\omega') \propto \frac{\exp\left[-\left(\frac{\omega-\omega'-\omega_{fo}(R_0)}{\gamma_f}\right)^2\right]}{(\omega' - \omega_{cf}(R_0))^2 + \Gamma_c^2}. \tag{25}$$

This equation can be written in the following simplified way which is often used in literature, namely

$$\sigma(\omega,\omega') \propto G(\Omega,\Omega',\Delta) \times L(\Omega',\Gamma), \tag{26}$$

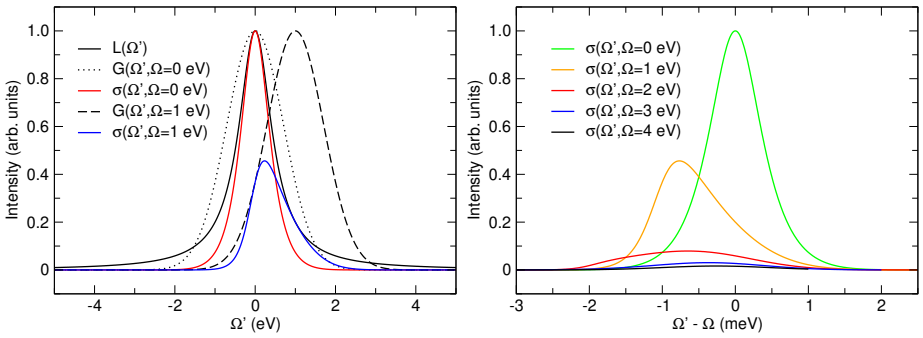

FIG. 2: Left: Lorentzian lineshape L for $\Gamma = 1$ eV, Gaussian lineshapes G for $\Delta = 1$ eV as well as $\Omega = 0$ eV and 1 eV, and resulting cross sections $\sigma(\Omega')$. Right: $\sigma(\Omega', \Omega)$ for $\Omega = 0$ to 4 eV.

i.e. it is the product of the Gaussian function

$$G(\Omega, \Omega', \Delta) = \exp\left\{-((\Omega' - \Omega)/\Delta)^2 \ln 2\right\} \tag{27}$$

and a Lorentzian function

$$L(\Omega', \Gamma) = \frac{1}{\Omega'^2 + \Gamma_c^2}. \tag{28}$$

Here $\Omega = \omega - \omega_{co}(R_0)$ is the difference between the photon energy $\omega$and the vertical transition energy $\omega_{co}(R_0)$ between the intermediate and the ground state, i.e. the small energy shift of $F\alpha$ is neglected. $\Omega' = \omega' - \omega_{fc}(R_0)$ is the deviation of the outgoing photon energy ω' from the energy difference of the potential energy curves of the intermediate and the final state $\omega_{fc}(R_0)$. Note that here ω_{fc} is independent of the the internuclear distance since the potential energy curves are assumed to be parallel, see above. Moreover, $\Delta = \sqrt{\ln(2)}\gamma_c$ is the HWHM of the Franck-Condon factor.

In the following we shall discuss the lineshapes resulting from eqn. 25. As can be seen in Fig. 2, the Lorentzian function is always centered around $\Omega' = 0$, i.e. its maximum is at the emitted photon $\omega' = \omega_{fc}(R_0)$. In contrast to this, the maximum of the Gaussian function does not only depend on ω' but also on the excitation energy ω. Instead, the maximum of the Gaussian function is at $\Omega' = \Omega$, i.e. it depend on the actual excitation energy ω. Since $\sigma(\omega, \omega')$ is a product of a Lorentzian with the maximum at $\Omega' = 0$ and a Gaussian with the maximum at $\Omega' = \Omega$ its maximum depends on the photon energy ω. This can be seen in Fig. 2. In the left part of this Figure we see the Lorentzian (solid black line) and two Gaussians for $\Omega = 0$ eV and 1 eV (dotted and dashed black line, respectively). Finally, the resulting cross sections for $\Omega = 0$ eV and 1 eV are represented by the solid red and blue lines, respectively. Note that the blue line shows a strong assymetry. In the right part of the figure cross sections for five different values of Ω can be seen. From these lineshapes it can be seen that (i) the peak position and (ii) the peak width changes with the photon energy. In more detail, the maximum is at $\Omega' - \Omega = 0$ eV for $\Omega = 0$ eV. Than it first increases with Ω, see $\Omega = 1$ eV. At higher values the deviation decreases again, see $\Omega = 2$ to 4 eV. Moreover, one sees also a complex behaviour for the linewidth (FWHM). This is minimal for $\Omega = 0$ eV and increase first with increasing Ω. At higher Ω (not seen here) the width decreases again and converges towards the the Frank-Condon width Δ. A detailed behavior these two quantities as a function of the photon energy is e.g. presented in [13].

In the following we will discuss the physical meaning of these lineshapes. For this, Figure 3 show a schematic picture of the RIXS process using a bound ground state in the harmonic approximation as well as a dissociative core-hole and final state in the linear approximation. Note that the dissociative character of the latter two states cause a continuum of nuclear wavefunctions each. For the ground state the nuclear wavefunction represented by a Gaussian distribution is shown in red. The blue curves represent Lorentzian distributions which are caused by the core-hole lifetime. Moreover, excitations and decays at three different internuclear distances are shown. For the middle transition the energy difference of the ground state and the core-hole state is equal to the photon energy ω. Because of this, the excitation probability is given by the product of the Franck-Condon factor for the corresponding internuclear distance and the maximum of the Lorentzian function. For the left and right transitions the photon energy is smaller and larger compared to the transition energy, respectively. Because of this the excitation probability governed by the Lorentzian function is reduced. In addition, the Franck-Condon factors are changed since the excitation occurs at a different internuclear distance. In summary, the probability of the transitions depend on the internuclear distance at which they take place and can be described by the product of a Lorentzian and a Gaussian function. By assuming that the internuclear distance does not change in the entire process and using the fact that the energy of the final state depends on the internuclear distance one obtains different energies ω' for the emitted photons.

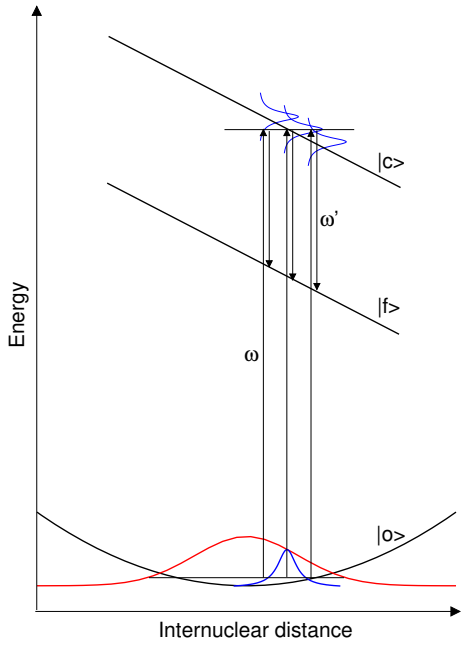

FIG. 3: Schematic picture to understand the lineshapes in the RIXS case. Given are the potential energy curves of a bound ground state $|o\rangle$ as well as the two dissociative states $|c\rangle$ and $|f\rangle$. The red Gaussian represents the vibrational wavefunction of the ground state. The blue lower Lorentzian indicates for a photon energy ω the internuclear distances at which the transition can take place with respect to energy conservation and the finite lifetime of the core-hole state. For more details, see text.

This now also allows to understand the non-linear dispersion typical for a bound-dissociative-dissociative process as shown e.g. in Fig. 6 of the main text. For the case that the Gaussian function is much broader than the Lorentzian function, see Fig. 3 it can readily be shown by simple simulations that the for small values of Ω the maximum of the product of the Lorentian and the Gaussian is close to the maximum of the Lorentzian. This means that for different photon energies around the resonance energy $\omega_{co}(R_0)$ the excitation process takes mainly place at different internuclear distances around the equilibrium distance. In more detail, the process takes place very close to that internuclear distance where the energy difference between the ground state and the intermediate state is equal to the photon energy ω. Since the resonant Auger decay always occurs at the same distance and since the potential energy curves are parallel, the emitted particle has the energy $\omega_{cf}(R_0)$, i.e. is not dependent on the photon energy ω. In contrast to this, for large detunings of Ω the maximum of the product of the Lorentian and the Gaussian is close to the maximum of the Gaussian. This means that the exciation takes place at the equilibrium distance. Because of this, the process ends at the same distance on the potential of the final state, i.e. $\omega' = \omega - \omega_{cf}(R_0)$ because of energy conservation. Consequently, ω' disperses linearly with ω.

It should be noted that Gel'mukhanov and Ågren investigated a mathematical identical case, however with different phyical quantities, and derive the non-linear behaviour of the dispersion analytically [12]. They investigate the energy positions and widths of atomic resonant Auger features as a function of the lineshape and the experimental resultion, where the lineshape is given by a product of a Lorentzian, see eqn. 5 and a Gaussian that represents the photon bandwidth.

C. The bound-dissociative-bound case

In the following we discuss the exotic case of a bound ground state, a bound final state and a dissociative intermediate state. This case is only realized in the shake-up process during the Auger decay. To describe this process we start again with equation 12 and assume an infinite lifetime of the final state. Moreover, we approximate the

core-hole state with $|\chi_c\rangle = \delta(R - (R_0 - \frac{\Delta E_c}{F_c}))$. In this way we obtain

$$\begin{aligned}\sigma(\omega,\omega') &\propto \sum_f \left| \frac{\int d\Delta E_c \langle\chi_f|\chi_c\rangle\langle\chi_c|\chi_0\rangle}{\omega - \omega_{co}(R_0) - \Delta E_c + i\Gamma_c} \right|^2 \delta(\omega - \omega' - \omega_{fo}(R_0) - \Delta E_f) \\ &= \sum_f \int d\Delta E_c \int d\Delta\tilde{E}_c \frac{\chi_f(R_0 - \frac{\Delta E_c}{F_c})\chi_0(R_0 - \frac{\Delta E_c}{F_c})}{[\omega - \omega_{co}(R_0) - \Delta E_c + i\Gamma_c]} \times \\ &\quad \frac{\chi_f(R_0 - \frac{\Delta\tilde{E}_c}{F_c})\chi_0(R_0 - \frac{\Delta\tilde{E}_c}{F_c})}{\left[\omega - \omega_{co}(R_0) - \Delta\tilde{E}_c - i\Gamma_c\right]} \times \delta(\omega - \omega' - \omega_{fo}). \end{aligned} \tag{29}$$

Here $\chi_0(R)$ and $\chi_f(R)$ are the vibrational wavefunctions of the bound intial and final state. The integrals $\int d\Delta E_c$ and $\int d\Delta\tilde{E}_c$ ensure that all possible intermediate core-excited states are taken into account. In case of a final state with finite lifetime we once again have to replace the δ-function by a Lorentzian function and obtain

$$\begin{aligned}\sigma(\omega,\omega') &\propto \sum_f \int d\Delta E_c \int d\Delta\tilde{E}_c \frac{\chi_f(R_0 - \frac{\Delta E_c}{F_c})\chi_0(R_0 - \frac{\Delta E_c}{F_c})}{[\omega - \omega_{co}(R_0) - \Delta E_c + i\Gamma_c]} \times \\ &\quad \frac{\chi_f(R_0 - \frac{\Delta\tilde{E}_c}{F_c})\chi_0(R_0 - \frac{\Delta\tilde{E}_c}{F_c})}{\left[\omega - \omega_{co}(R_0) - \Delta\tilde{E}_c - i\Gamma_c\right]} \times \frac{1}{(\omega - \omega' - \omega_{fo})^2 + \Gamma_f^2}. \end{aligned} \tag{30}$$

D. The bound-dissociative-bound case

The last case we want to discuss is the bound-bound-dissociative case. By already assuming a finite lifetime for the final state and the arguments given above we obtain

$$\sigma(\omega,\omega') \propto \int d\Delta E_f \left| \sum_c \frac{\langle\chi_f|\chi_c\rangle\langle\chi_c|\chi_o\rangle}{\omega - \omega_{co} + i\Gamma_c} \right|^2 \times \frac{1}{(\omega - \omega' - \omega_{fo})^2 + \Gamma_f^2}. \tag{31}$$

The overlap matrix elements $\langle\chi_c|\chi_o\rangle$ for the bound-bound excitation can be calculated given by the method described in section II A. The matrix elements $\langle\chi_f|\chi_c\rangle$ can be obtained by following the method described in section II B. In detail, for the matrix element $\langle\chi_f|0_c\rangle$ eqn. 19 can be used. For higher vibrational levels in the core-hole state we refer to Püttner et al. [7].

IV. COMPARISON OF EXPERIMENTAL AND SIMULATED PARTIAL ELECTRON YIELD SPECTRUM

In Fig. 4 a direct comparison of the simulated and the experimental electron yield is given and shows a good agreement.

[1] F. Gel'mukhanov *et al.*, Phys. Rev. A, **54**, 379 (1996).
[2] H. A. Ory, A. P. Gittleman, and J. P. Maddox, Astrophys. J. **139**, 346 (1964).
[3] M. Halmann and I. Laulich, J. Chem. Phys. **43**, 438 (1965).
[4] R. Püttner, I. Dominguez, T. J. Morgan, C. Cisneros, R. F. Fink, E. Rotenberg, T. Warwick, M. Domke, G. Kaindl, and A. S. Schlachter Phys. Rev. A **59**, 3415 (1999).
[5] O. Vallee and M. Soares, *Airy Functions and Applications to Physics (2nd Edition)* (Imperial College Press, London, 2010), pp. 147.
[6] G. Herzberg, *Molecular Spectra and Molecular Structure I. Spectra of Diatomic Molecules* (Van Nostrand, NewYork, 1950), p. 393.
[7] R. Püttner, T. Arion, M. Förstel, T. Lischke, M. Mucke, V. Sekushin, G. Kaindl, A. M. Bradshaw, and U. Hergenhahn, Phys. Rev. A **83**, 043404 (2011).
[8] Ref. [5], page 56.

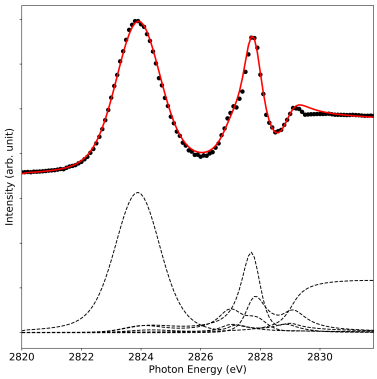

FIG. 4: Experimental and simulated partial electron yield represented by the black data points and the red solid line, respectively. The dashed subspectra below the lines indicate the direct contibutions of the individual final-state cross sections.

[9] R. Püttner, Y. F. Hu, G. M. Bancroft, H. Aksela, E. Nõmmiste, J. Karvonen, A. Kivimäki, and S. Aksela Phys. Rev. A **59**, 4438 (1999).
[10] R. Püttner, V. Pennanen, T. Matila, A. Kivimäki, M. Jurvansuu, H. Aksela, and S. Aksela Phys. Rev. A **65**, 042505 (2002).
[11] T. Marchenko *et al.*, Phys. Rev. Lett. **119**, 133001 (2017).
[12] F. Gel'mukhanov and H. Ågren, Phys. Rev. A **54**, 3960 (1996).
[13] M. Simon, L. Journel, R. Guillemin, W. C. Stolte, I. Minkov, F. Gelmukhanov, P. Salek, H. Ågren, S. Carniato, R. Taïeb, A. C. Hudson, and D. W. Lindle, Phys. Rev. A **73**, 020706(R) (2006).
[14] P. M. Morse, Phys. Rev. **34**, 57 (1929).